Supporting Online Material for

Body-Centered Cubic Iron-Nickel Alloy in Earth's Core

L. Dubrovinsky, N. Dubrovinskaia, O.Narygina, I. Kantor, A. Kuznetzov, V. B. Prakapenka, L. Vitos, B. Johansson, A. S. Mikhaylushkin, S. I. Simak, I. A. Abrikosov

Published 29 June 2007, *Science* **316**, 1880 (2007)
DOI: 10.1126/science.1142105

This PDF file includes:

Supporting Online Material for

Body-Centred-Cubic Iron-Nickel Alloy in the Earth's Core

L. Dubrovinsky*, N. Dubrovinskaia, O.Narygina, I. Kantor, A. Kuznetzov, V. Prakapenka, L. Vitos, B. Johansson, A. S. Mikhaylushkin, S. I. Simak, I. A. Abrikosov

*To whom correspondence should be addressed. E-mail: Leonid.Dubrovinsky@uni-bayreuth.de

This PDF file includes:

Experimental pressure scale

The absolute values of the pressure and estimates of the changes of density between different phases and/or compounds (particularly pure Fe and Fe-Ni alloys) depend on the adopted pressure scale and the hcp-Fe equation of state (EOS). Dewaele et al. (*S1*) and Dubrovinsky et al. (*S2*) give quite different EOS of hcp-Fe. For example, at 300 K and given molar volume 4.5 cm^3/mole, the corresponding pressures are 187 GPa and 198 GPa. A probable reason of the inconsistency is the use of different pressure scales (calibrants) – W (*S3*) in paper by Dewaele et al. (*S1*) and Pt (Holmes et al.; see Ref. 14 (*S2*)). Direct comparison of the EOS is difficult, but fortunately Dewaele et al. (Ref. *S3*) presents data on both tungsten and platinum collected, processed, and treated in the same self-consistent way. It opens for us a possibility to "re-calibrate" pressures obtained in Dubrovinsky et al. (*S2*) and Mao et al. (*S4*) works from Pt pressure calibrant and compare with the data reported by Dewaele et al. (*S1*). As shown in Fig. S1, there is perfect agreement between all data sets. It allows us to apply similar corrections when comparison between data obtain in this work and data reported by Dewaele et al. (*S1*) was necessary.

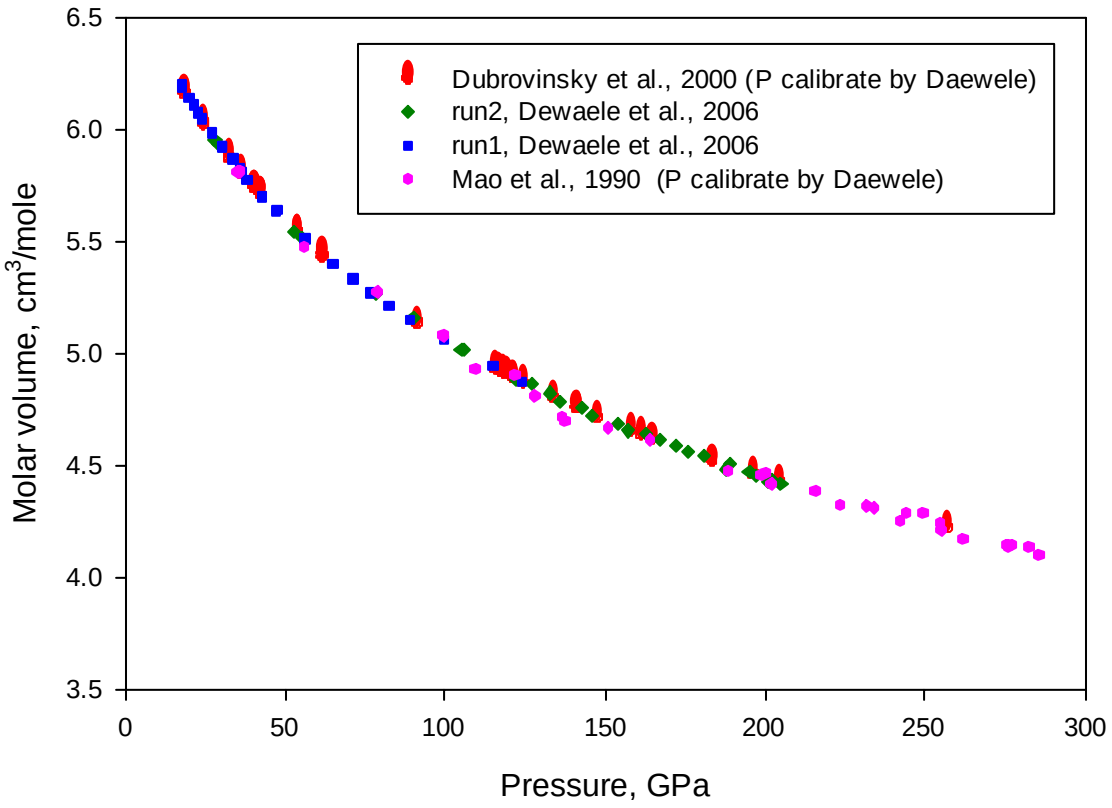

Fig. S1. Comparison between molar volumes of hcp Fe at ambient temperature measured by Dewaele et al. (*S1*) (original data) and Dubrovinsky et al. (*S2*) and Mao et al. (*S4*) (pressure scale corrected according to Dewaele et al. (Ref. *S3*).

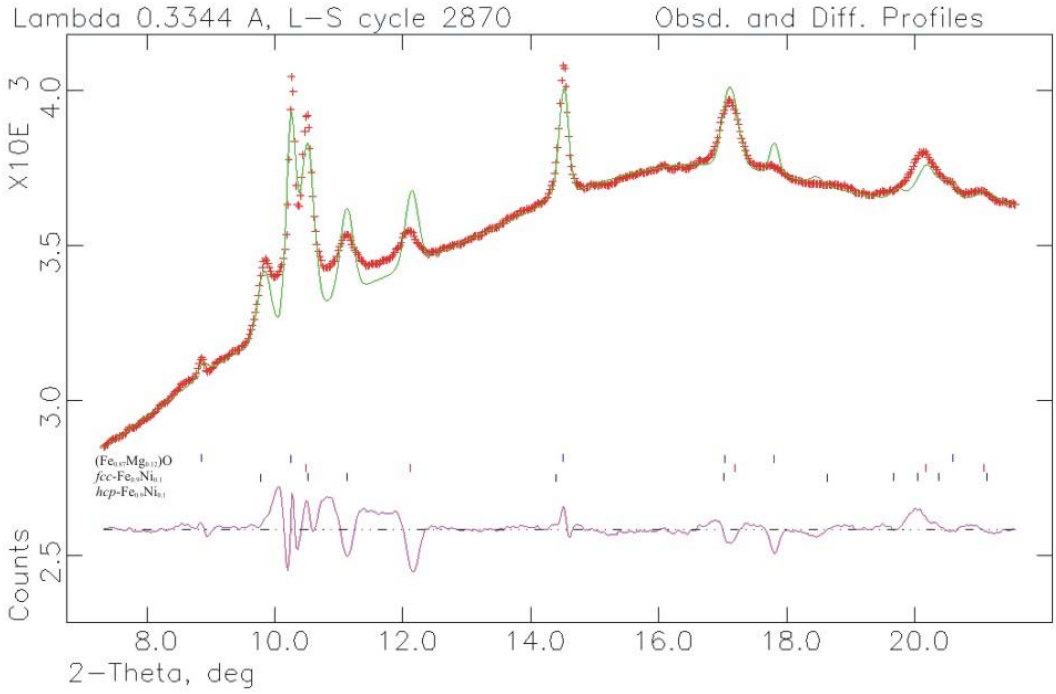

Fig. S2. Example of full-profile treated diffraction pattern collected at 132(10) GPa and 3100(100) K.

Theoretical Simulations

Phonon dispersion relations in bcc Fe and $Fe_{0.9}Ni_{0.1}$

Theoretical calculations of the phonon dispersion relations in pure bcc Fe and $Fe_{0.9}Ni_{0.1}$ alloy were carried out in the framework of the density functional theory (*S5*) using the generalized gradient approximation (GGA) for the exchange-correlation energy and one-electron potential (*S6,S7*). We used the Projector Augmented-Wave (PAW) (*S6*) method as implemented in Vienne Ab initio Simulation Package (VASP) (*S11,S12*). The PAW technique allows us to investigate the dynamical behavior of the Fe-Ni alloys within the so-called Virtual Crystal Approximation (VCA) (*S13*). Though less accurate than the coherent potential approximation (CPA) (*S8*), VCA is known to work well for alloys between neighboring elements in the Periodic Table (*S13,S14*).

The PAW-VCA calculations were carried out within the frozen core approximation. The energy cut-off was set to 366.6 eV. The 4s, 4p, 3d, as well as 3p-semicore states of Fe and Ni were treated as valence. The integration over the Brillouin zone was performed on a grid of special k-points determined according to the Monkhorst-Pack scheme (*S15*). The finite temperature calculations of the electronic structure, electron entropy, and forces needed to calculate phonon spectra were carried out within the Fermi-Dirac-smearing approach (*S16*). Phonon-frequency calculations were carried out in the framework of the supercell approach (Small Displacement Method) described in detail in Ref. *S17*.

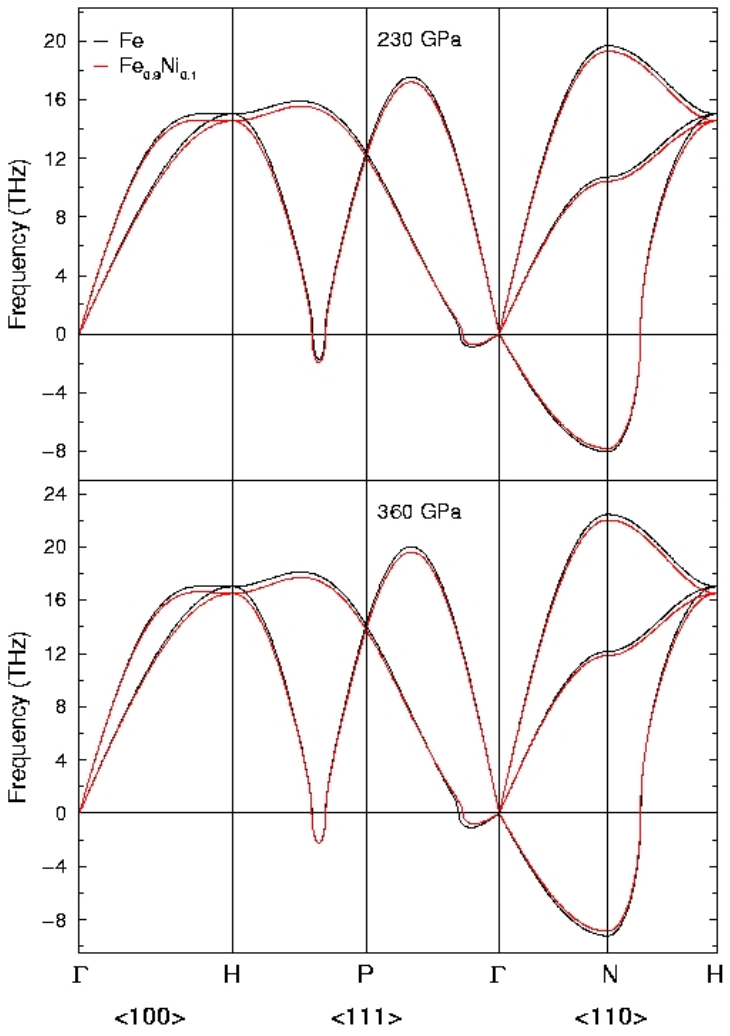

Fig. S3. Phonon dispersion curves for bcc Fe (black line) and bcc $Fe_{0.9}Ni_{0.1}$ alloy (red line) along the high symmetry lines of the bcc Brillouin zone calculated by the PAW-VCA method in the (quasi)-harmonic approximation with forces obtained at T=5000 K. For a stable structure, all vibrational frequencies ω, obtained from the eigenstates ω^2 of the determinant equation (*S19*), must be positive. Dispersion curves at negative frequencies correspond to imaginary ω values for the points in the Brillouin zone where ω^2 are negative, indicating the dynamical instability of the bcc phase in the (quasi)-harmonic approximation. Note that the effect of Ni on the phonon properties of bcc $Fe_{0.9}Ni_{0.1}$ alloy is very small.

Energetic effect of the Ni substitution into bcc and hcp Fe

The all-electron calculations of the alloying effect on the total energy and elastic properties of pure Fe and Fe-Ni alloys were carried out within the Exact Muffin Tin Orbital (EMTO) theory (*S17*) and the density functional theory (*S7*) using the generalized gradient approximation (GGA) for the exchange-correlation energy and one-electron potential (*S8*). The EMTO method is combined with the coherent potential approximation (CPA) (*S13*,*S17*), which allows for the most accurate treatment of disorder effects in random substitutional alloys, including calculations of the mixing energies and elastic constants (*S16*).

3d and *4s* electrons of Fe and Ni were treated as valence electrons and the core states were relaxed after each iteration. We checked the influence of including *3p* semi-core states in the valence band, and find that in all-electron EMTO calculations this has negligible effect on the energetics and elastic properties of Fe-Ni alloys up to pressure of at least 400 GPa. A sufficiently dense mesh was used for calculating reciprocal space and energy integrals, so that the total energy was converged to within 0.1 meV. The finite temperature calculations of the electronic structure and electron entropy were carried out in the quasi-harmonic approximation using the Fermi function smearing. Dependences of the total energy on the volume for each system were fitted using the Birch-Murnaghan equation, and theoretical values of pressure were calculated from the fit.

The energetic effect of the Ni substitution into bcc and hcp Fe was calculated according to the methodology suggested in Ref. *S18*. The obtained stabilization energy of the bcc phase relative to the hcp phase due to the alloying of Fe with Ni is shown in Fig. S4. Calculated elastic constants *c'* for pure bcc Fe and $Fe_{0.9}Ni_{0.1}$ alloy are given in the text.

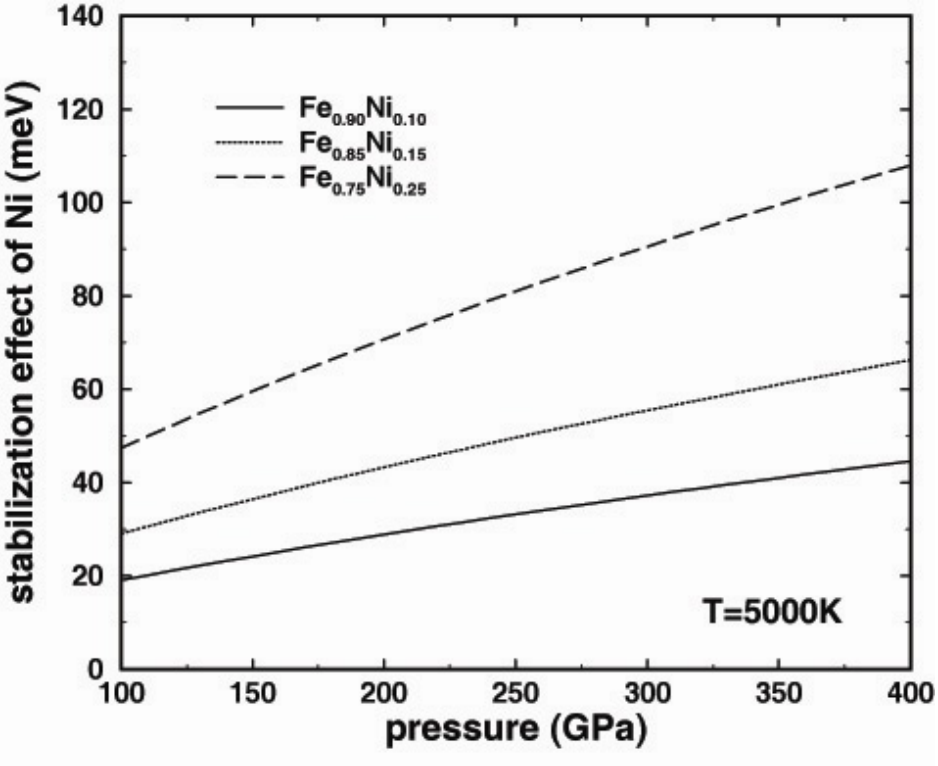

Fig. S4. Calculated energetic effect of the Ni substitution into bcc and hcp Fe as a function of pressure and Ni composition. The curves show the stabilization energy (*S18*) of the bcc phase relative to the hcp phase due to the alloying of Fe with Ni calculated using the EMTO-CPA method. Calculations include the temperature effects on the electronic structure simulated by the Fermi-distribution, as well as the electron entropy term. Note that large-scale molecular dynamics simulations based on the embedded atom model (*S19*) predicted that the bcc phase of pure Fe was already more stable than the hcp phase at the Earth's core conditions. The first-principles molecular dynamics simulations for supercells of moderate size (*S18*) showed that the bcc phase of pure Fe was less stable thermodynamically (by 33-58 meV) than the hcp phase, but it could be stabilized at the Earth's core pressures and temperatures if silicon or sulfur impurities are present. These results have been supported by experimental findings of ordered and possibly disordered bcc-structured Fe-Si alloys at pressures above 140 GPa and high temperatures (*S20,S21*) Our first-principles results show that Ni stabilizes the disordered bcc phase relative to the hcp phase. In particular, 10 at. % of Ni stabilizes the bcc phase by 32 meV at a pressure of 230 GPa and by 41 meV at 350 GPa, as compared to pure Fe. This effect of bcc

stabilization clearly increases with increasing Ni concentration and pressure, and it can be explained from simple band filling arguments. Indeed, the so-called canonical band structure calculations (S22) show that non-magnetic phase of the bcc Fe is located very close to the maximum of the bcc-hcp energy difference curve plotted as a function of the *d*-band occupation. Alloying with Ni increases the *d*-band filling, leading to a relative stabilization of the bcc phase in Fe-Ni alloys.

References

S1. A. Dewaele, P. Loubeyre, F. Occelli, M. Mezouar, P. I. Dorogokupets, M. Torrent, *Phys. Rev. Lett.* **97**, 215504 (2006)

S2. L. S. Dubrovinsky, S. K. Saxena, F. Tutti, T. Le Bihan, *Phys. Rev. Lett.* **84**, 1720-1723 (2000).

S3. A. Dewaele, P. Loubeyre, M. Mezouar, *Phys. Rev. B* **70**, 094112 (2004)

S4. H. K. Mao, Y. Wu, L. C. Chen, J. F. Shu, A. P. Jephcoat, *J. Geophys. Res.* **95,** 21737-21742 (1990).

S5. Hohenberg, P. & Kohn, W. *Phys. Rev.* **136B**, 864-871 (1964).

S6. Perdew, J. P., Burke, K. and Ernzerhof, M. Phys. Rev. Lett **77**, 3865 (1996).

S7. Wang Y. and Perdew, J.P. Phys. Rev. **44**, 13298 (1991)

S8. Blöchl, P. E., *Phys. Rev. B* **50,** 17953-17979 (1994).

S9. Kresse, G. & Hafner, J. *Phys. Rev. B* **48,** 13115-13118 (1993).

S10. Kresse, G. & Furthmüler, J. *Comput. Mater. Sci.* **6**, 15-50 (1996).

S11. Faulkner, J. S. Prog. Mater. Sci. **27**, 1 (1982)

S12. Abrikosov, I. A., James, P., Eriksson, O., Söderlind, P., Ruban, A. V., Skriver, H. L. and Johansson, B., Phys. Rev. B **54**, 3380-3384 (1996).

S13. Monkhorst, H. J. and Pack, J. D. Phys. Rev. B 13, 5188- 5192 (1976).

S14. Mermin, N.D. Phys. Rev. **137**, A 1441(1965).

S15. Kresse, G. and Furthmüler, J. Europhys. Lett. 32, 729-734 (1995).

S16. Andersen, O. K., Jepsen, O. and Krier, G., in *Lectures on Methods of Electronic Structure Calculations, edited by Kumar, V., Andersen, O. K. and Mookerjee, A. World Scientific Publishing Co., Singapore.* 63-124 (1994).

S17. Vitos, L., Abrikosov, I. A., & Johansson, B. *Phys. Rev. Lett.* **87**, 156401 (2001).

S18. L. Vocadlo, D. Alfe, M. J. Gillan, I. G. Wood, J. P. Brodholt, G. D. Price, *Nature* **424**, 536-539 (2003).

S19. A. B. Belonoshko, R. Ahuja, and B. Johansson, *Nature* **424**, 1032-1034 (2003).

S20 J.-F. Lin, D.L. Heinz, A. J. Campbell, J. M. Devine, G. Shen, *Science* **295,** 313-315 (2002).

S21. L. Dubrovinsky, N. Dubrovinskaia, F. Langenhorst, D. Dobson, D. Rubie, C. Geshmann, I. A. Abrikosov, B. Johansson, V. I. Baykov, L. Vitos, T. Le Bihan, W. A. Crichton, V. Dmitriev, and H.-P. Weber, *Nature* **422,** 58-61 (2003).

S22. H. L. Skriver, *Phys. Rev. B* **31**, 1909-1923 (1985).